

Design and Comparison analysis of Fuzzy and ANN based MPPT Controller

Shreedevi K V¹, DR K P Shashikala²

¹Shreedevi K V [1] PG student, Department of ECE, DSCE, Bangalore, India

²DR.K P Shashikala Professor, Dept. of ECE, DSCE, Bangalore, India

Abstract - In this paper, a PV (Photovoltaic) power sourced battery charging unit (boost and buck converter) was designed for maximum power point tracking (MPPT) and extraction of PV power and performs battery charging under constant voltage (CV) mode using voltage mode control circuit operating on the buck converter. The fuzzy logic controller and Artificial Neural Network controller are introduced as MPPT controller and the efficiency of the converter under these controllers are measured and compared. Simulation work is carried out in MATLAB/Simulink software which determines its maximum power point tracking performance.

Key words—Photovoltaic source, dc-dc converters, fuzzy logic controller, artificial neural network, battery charging techniques.

1. INTRODUCTION

Traditional energy sources such as fossil fuels are going scarce compared to the growing demands and also it leads to more pollution. The renewable energy sources such as PV is adapted due to low operating cost and as the power generation process is free of any pollution. But it is less efficient and non reliable due to frequent changes in weather conditions. To make it more efficient MPPT techniques such as Perturb and Observe (P&O), Incremental conductance algorithms are developed for single PV panel systems. These algorithms track the maximum PV power and corresponding voltage, so that it makes the converter operates on that particular voltage and extracts the maximum power. The converters such as boost, buck sepic, buck-boost, buck, etc., are used for extracting maximum power from PV system with the help of MPPT controller. The above mentioned MPPT algorithms is implemented with FLC and ANN controllers so that it can be more efficient, accurate and quicker in response to the changes in environmental conditions such as irradiance, temperature, etc., The PV power is utilized in order to feed the grid or standalone loads or to charge the battery which is used for later utilization. The battery charging by the PV source faces difficulties when the irradiation is reduced as the voltage and power generated by the PV panel gets reduced with

irradiation. When it reduced further below the battery voltage, there will be no charging which reduces the efficiency of the system. Even with MPPT, the voltage variations are unavoidable and hence unsuitable for battery charging applications. The battery can be charged under varying PV voltage or power using the following controllers:

- i) Constant Voltage (CV) control and
- ii) Constant Current (CC) control

Constant current control is more efficient for battery charging applications but appropriate voltage ($>V_{\text{battery_minimum}}$) also should be maintained to charge the battery with reduced loss and also to charge the battery quickly so that the lifetime of battery is increased. It is difficult for lesser irradiations and hence constant voltage technique is used in this scenario. To provide constant voltage, PI controller is used for providing the pulses to the converter. The performance curves of both current and voltage control techniques are provided in Fig. 1

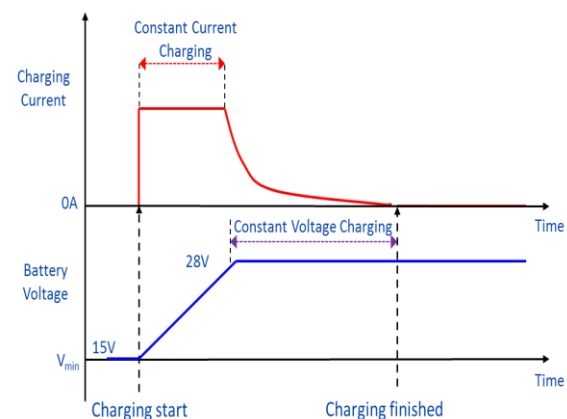


Fig. 1. Constant voltage and constant current control performance curves

In this paper, the PV panel of 60V/720W is subjected to the FLC and ANN based MPPT control and the efficiency of the two controllers is compared under varying irradiation. The PI controller based constant voltage circuit is used to provide switching pulses for buck converter in order to charge the battery. The design procedure of the converters and the MPPT controllers are provided in this paper.

2. MODELLING OF PHOTOVOLTAIC CELL

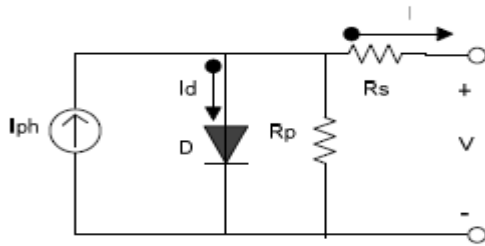


Fig. 2. Equivalent circuit of single diode model of PV cell

In various literatures it is also termed as a five parameter model (I_{ph} , I_o , n , R_s and R_p).

Where

I_{ph} - Photocurrent (A)

I_o - Diode saturation current (A)

n - Diode factor ($1 \leq n \leq 2$)

R_s - Series resistance (Ω)

R_p - Shunt resistance (Ω)

- R_s is used to represent internal current flow losses and voltage drops.

- R_p is used to measure the internal leakage current flow due to reverse biasing of diode.

$$I = I_{ph} - I_o \left(e^{\frac{V+IR_s}{n_s V_T}} - 1 \right) - \frac{V+IR_s}{R_p} \quad (1)$$

3. PV FED BATTERY CHARGING UNIT

The proposed PV fueled battery charging unit is provided in Fig. 3.

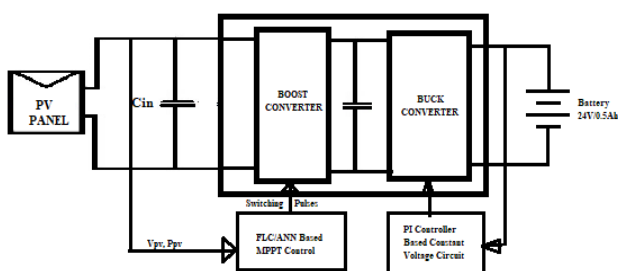


Fig. 3. Proposed PV fed battery charging unit

The PV power is provided to boost converter which steps up the PV voltage according to the duty ratio generated by the FLC or ANN based MPPT controller and the boosted voltage is reduced to battery voltage or the reference voltage provided for PI controller based voltage control circuit by the buck converter.

The circuit for boost converter is provided in Fig. 4.

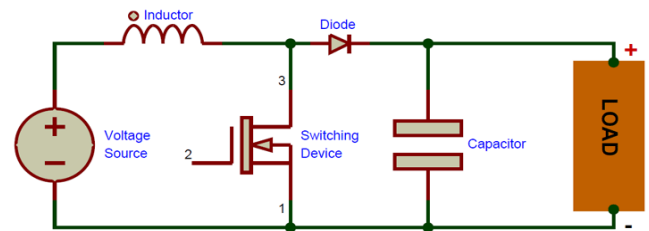


Fig. 4. Boost Converter circuit

The boost converter is used to step-up the dc voltage according to the duty ratio of the switching pulse provided. It comprises of inductor, power electronic switch, diode and capacitor. The load voltage will be higher than that of input voltage. The operational modes of the boost converter are provided as follows:

Mode 1:

The mode1 operational circuit is provided in Fig. 5. Here, the gate pulse provided for switch S is HIGH and the inductor gets charged during this time period. The capacitor, will maintain the load voltage at designed value during this time period. The inductor voltage and load voltage are provided in the following equations:

$$V_L = V_{in} \quad V_{Co} = V_o$$

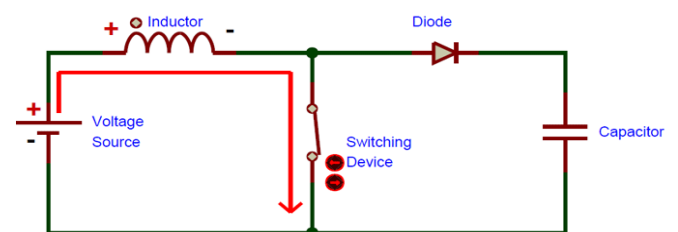


Fig. 5. Mode 1 Equivalent circuit of boost converter, $V_L=V_{in}$

Mode 2:

The mode2 operational circuit is provided in Fig. 6. Here, the gate pulse provided for switch S is LOW and the inductor gets discharged during this time period. The inductor voltage and source voltage gets added and provided

to the load. The load voltage is provided in the following equation:

$$V_o = V_L + V_{in}$$

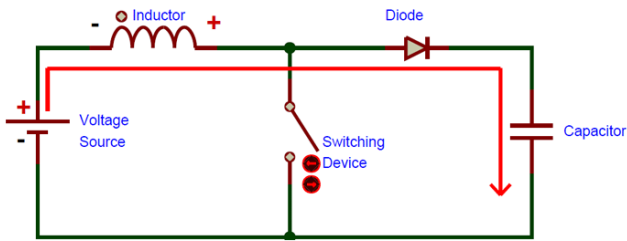


Fig.6 .Mode 2Equivalent circuit of boost converter, $V_o=V_{in}+V_L$

The buck converter circuit is provided in Fig. 7.

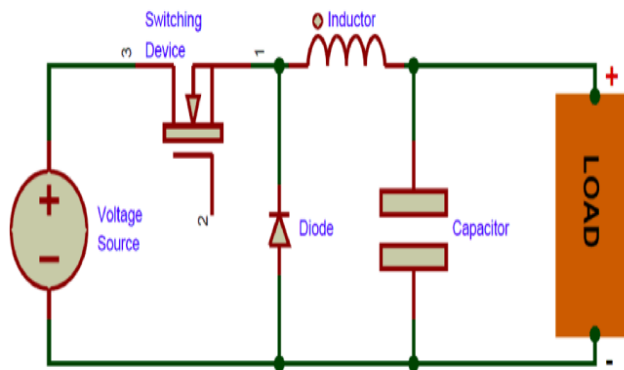


Fig.7.Buck converter circuit

The buck converter is used to step-down the dc voltage according to the duty ratio of the switching pulse provided. It consists of an inductor, switch, diode and capacitor. The load voltage will be lower than that of input voltage. The operational modes of the buck converter are provided as follows:

Mode 1:

The mode1 operational circuit is provided in Fig. 8. Here, the gate pulse provided to switch S is HIGH and the inductor gets charged during this time period. The inductor voltage and load voltage are provided in the following equations:

$$V_o = V_{in} - V_L$$

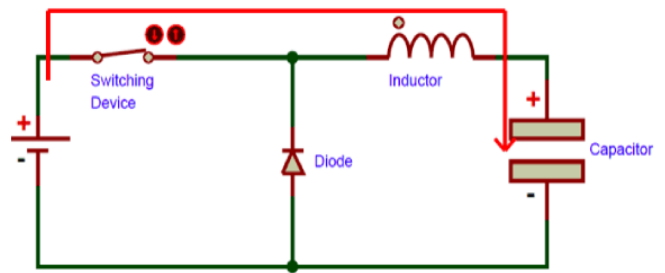


Fig. 8. Mode 1Equivalent circuit of buck converter, $V_o=V_{in}-V_L$

Mode 2:

The mode2 operational circuit is provided in Fig. 9. Here, the gating pulse provided for the switch, S is LOW and the inductor gets discharged during this time period. The load voltage is provided in the following equation:

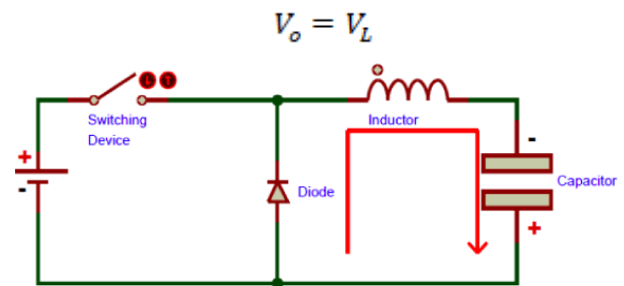


Fig. 9. Mode 2Equivalent circuit of buck converter, $V_o=V_L$

4. DESIGN OF FUZZY LOGIC CONTROL

Fuzzy inference system is the main component of fuzzy logic system whose primary function is decision making. The functional diagram of fuzzy logic controller is provided in Fig 10.

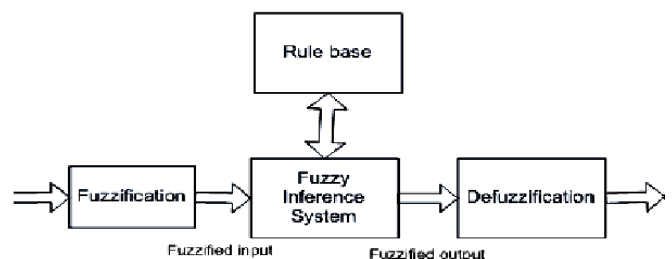


Fig.10.Functional block diagram of Fuzzy Logic Controller

Fuzzy inference system process comprises of following procedures:

- Input variables are processed and undergoes the Fuzzification step

- Applying the fuzzy operator (AND or OR) process as per the rules.
- Defuzzification of the fuzzy outputs

The rules provided for the FLC controller is provided in Table I as shown below:

TABLE I Rules of the FLC control

$\Delta P/\Delta V$	NVL	NL	NM	NS	Zero	PS	PM	PL	PVL
NVL	PVL	PL	PM	PM	PM	NL	NL	NVL	NVL
NL	PVL	PL	PM	PM	PM	NM	NL	NVL	NVL
NM	PL	PL	PM	PM	PS	NM	NM	NL	NL
NS	PM	PM	PS	PS	Zero	NS	NM	NM	NM
Zero	PS	PS	PS	Zero	Zero	Zero	NS	NM	NM
PS	Zero	Zero	Zero	NS	Zero	Zero	Zero	PS	PM
PM	NS	NS	NS	NS	NS	PS	PM	PM	PL
PL	NM	NM	NM	NM	NM	PM	PL	PL	PVL
PVL	NL	NL	NL	NL	NL	PL	PL	PVL	PVL

The MPPT controller will provide the change in duty ratio(ΔD) which will be added with initial duty ratio and provided for pwm pulse generation unit. The pulse generated is given to the gate terminal of the boost converter switch. Both the FLC and ANN control operates under the following conditions:

If $\Delta P/\Delta V > 0$, ΔD is +ve, [22]

If $\Delta P/\Delta V < 0$, ΔD is -ve. [22]

5. DESIGN OF ANN CONTROL

The ANN senses the change in voltage and power and generates the duty ratios as per the equations (2) and (3). Hence if there is change in irradiation, the ANN control is accurate and quicker in response than any other control and provides the appropriate duty ratio in order to extract maximum PV power. The training was done with the help of data taken from the base system. The Levenberg-Marquardt algorithm used for training the neural network. This algorithm requires more memory but minimum time. Training will stop when improvement of generalization stops, as indicated by an increase in the mean square error of the validation samples. The fitting curve of the training of ANN controller is provided in the following graphs (Fig. 11):

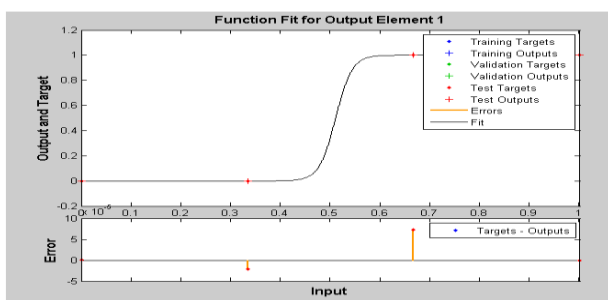


Fig. 11.Fitting curves from neural network training

The regression value obtained from the training of neural network control is 0.99953. The regression curve is provided in the following graphs (Fig 12):

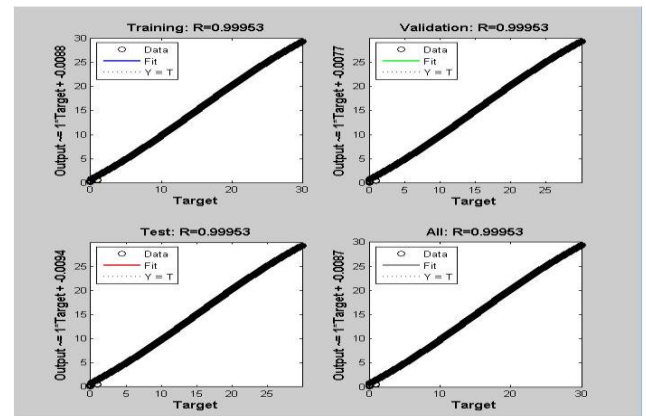


Fig. 12. Regression curves from neural network training

6. CONSTANT VOLTAGE CONTROL LOOP

The proposed voltage mode controller block diagram is shown in Fig 13. The reference voltage compared with the measured voltage and the error voltage generated is provided to PI controller. The PI controller provides the duty ratio for buck converter so that the error voltage is to be reduced and reached zero.

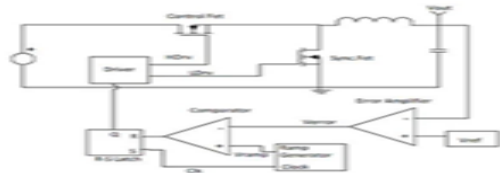


Fig. 13.Constant voltage control circuit for Buck converter

The transfer function of PI controller is provided below:

$$G_{pi}(s) = K_p + K_i/S \quad [22]$$

7. BOOST & BUCK CONVERTER DESIGN EQUATIONS

The design of boost converter circuit is provided by following equations:

The Duty ratio (D) of the boost converter circuit is provided below:

$$D = \frac{V_o}{V_o - V_{in}}$$

The inductor value of the boost converter circuit is calculated by the following equation:

$$L/2 = \frac{V_{in} * D}{\Delta I_o * F_{sw}}$$

The inductor ripple current is selected using the following equation:

$$\Delta I_L = 0.2 * \frac{V_o}{V_{in}} * I_o$$

The output capacitance of the boost converter circuit is given by the following equation:

$$C_o = \frac{\Delta I_{oc}}{8 * F_{sw} * \Delta V_o}$$

The capacitor ripple voltage is selected from the following equation:

$$\Delta V_{oc} = 2\% \text{ of } V_o$$

The design of the buck converter circuit is provided by the following equations:

The Duty ratio (D) of the buck converter circuit is provided below:

$$D = \frac{V_o}{V_{in}}$$

The inductor value of the buck converter circuit is calculated by the following equation:

$$L = \frac{V_o * (V_o - V_{in})}{\Delta I_o * F_{sw} * V_{in}}$$

The inductor ripple current is selected using the following equation:

$$\Delta I_L = 0.2 * I_{in}$$

The output capacitance of the buck converter circuit is given by the following equation:

$$C_o = \frac{\Delta I_{oc}}{8 * F_{sw} * \Delta V_o}$$

The capacitor ripple voltage is selected from the following equation:

$$\Delta V_{oc} = 2\% \text{ of } V_o$$

8. SIMULATION SETUP AND RESULTS

The simulation circuit parameters are provided in Table II as follows:

TABLE II Simulation Parameters

Parameters	Values
PV Voltage	60V
PV Power	700W
Boost converter Output voltage	110V
Battery Voltage	24V
Switching Frequency	5KHZ
Inductors	L _{Boost} = 3.2mH L _{Buck} = 0.76mH
Capacitors	C _{Boost} = 372µF C _{Buck} = 520µF

The simulation circuit of the PV fed battery charging converters is provided in Fig 14.

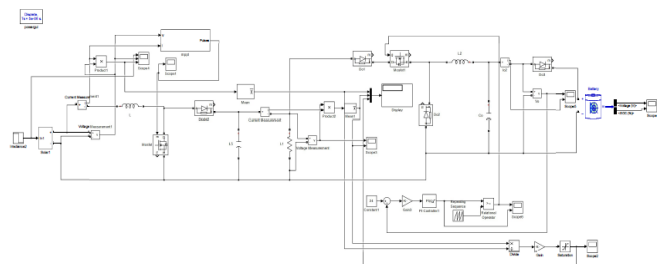


Fig.14.Simulation circuit of the PV fed battery charging converter

In this, the irradiation is initially 1000W/m2 and at t=0.2s, the irradiation changed to 600W/m2. Due to this reduction in irradiation, the PV voltage and power is also gets reduced. The change in PV voltage and power due to change in solar irradiation is provided in the graph shown in Fig. 15.

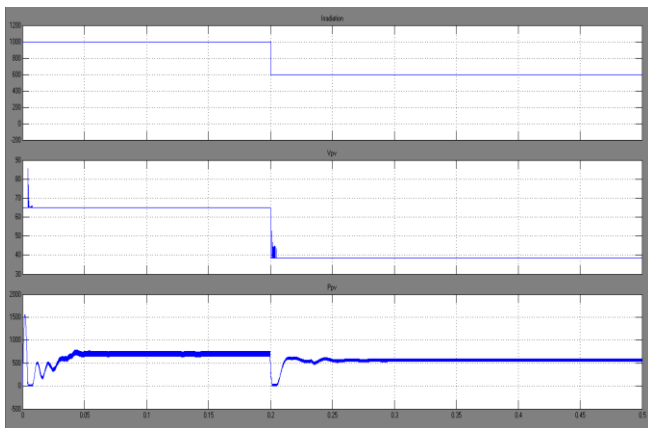


Fig.15.PV voltage and power for different irradianations

The MPPT controller is provided with PV voltage and power and based on the change in voltage and power, the mppt controller extracts the maximum possible power with the help of FLC and ANN tools. The simulation circuit for the MPPT is provided in Fig. 16.

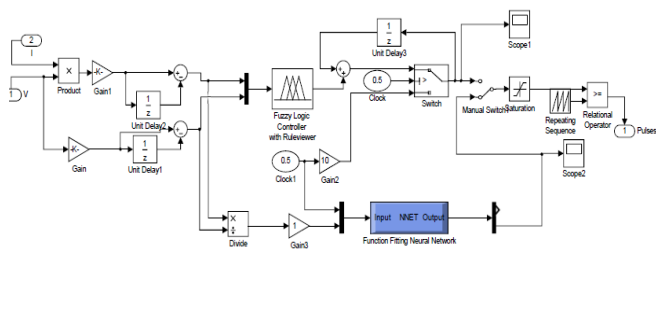


Fig.16.Simulation circuit of the FLC and ANN based MPPT controller

The MPPT controller senses the change in power generated by PV panel and updates the duty ratio in order to extract maximum possible power at given conditions. The change in duty ratio generated from the MPPT controller is provided in the graph shown in Fig. 17.

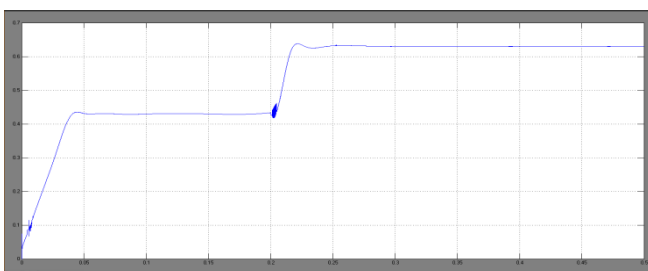


Fig.17.Duty Ratio generated with the help of MPPT controller

The duty ratio generated from MPPT is provided to pulse generation circuit which generates the gating pulses for the boost converter switch. Based on the gating pulses, the output voltage of boost converter is varied. The output voltage and power waveforms of the boost converter are provided in the graph shown in Fig. 18.

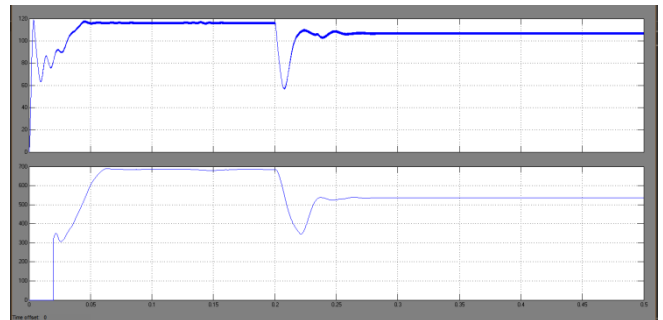


Fig.18.Boost converter output voltage and power

The efficiency of the MPPT controller is provided in the graph shown in Fig 19.

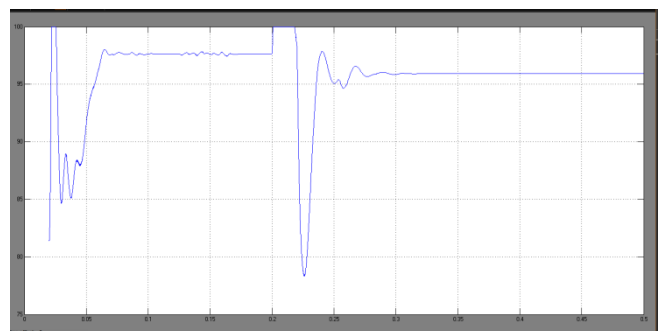


Fig.19. %Efficiency of the MPPT controller

The efficiency measured from the above graph is 97.6% for Irradiation of 1000W/m² and 96% for irradiation of 600W/m².The boost converter output is provided as buck converter input. The variations in the output voltage of boost converter are regulated to battery voltage of 24V with the help of voltage mode control circuit with PI controller. The Kp and Ki values of the PI controller is 0.9 and 0.1 respectively. The battery voltage and %SOC is provided in the graph shown below in Fig. 20.

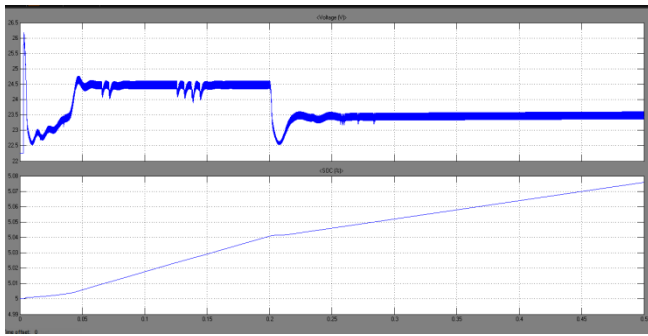


Fig.20. Battery voltage and %SOC

The rate of charging of the batteries differs when the PV irradiation is changed which can be seen in the %SOC waveform in the above graph.

The performance comparison of FLC and ANN based MPPT controllers for different irradiances are provided in Table III as shown below:

TABLE III Comparative Analysis of Performance of FLC and ANN based MPPT Controllers

Parameters	Irradiation = 1000 W/m ²		Irradiation = 600W/m ²	
	FLC	ANN	FLC	ANN
V _{pv} (V)	65	65	39	39
P _{pv} (W)	700	700	490	495
V _o (V)	110	115	98	105
%Efficiency	97.5	97.6	95.5	96

The %efficiency of ANN and FLC controllers are almost same for maximum irradiation 1000W/m² and as the irradiation reduces, then the %efficiency of ANN is higher than that of FLC controller.

9. CONCLUSION

In this paper, PV sourced battery charging circuit was designed along with FLC and ANN based MPPT controllers. The boost and buck converters are analyzed and designed with PV as input and battery as load. PI controller based constant voltage control circuit was designed to provide load regulation with varying PV voltage conditions. The efficiency of FLC and ANN controllers are measured and compared for different solar irradiances. The proposed system consists of single PV panel and for multiple PV panels, the design of FLC and ANN based MPPT controller is to be modified so that it is also suited for partial shading conditions.

REFERENCES

- [1] V. M. Elena and Papadopoulou, "An environmental approach," Green Energy and Technology, Springer Heidelberg Dordrecht London New York, 2011.
- [2] L. Zaghba, N. Terki, A. Borni, and A. Bouchakour, "Intelligent control MPPT technique for PV module at varying atmospheric conditions using matlab/simulink," Proc. of IEEE International Renewable and Sustainable Energy Conference (IRSEC), DOI: 10.1109/IRSEC.2014.7059793, ISBN: 978-1-4799-7336-1, 17-19 October, 2014, pp. 661-666.
- [3] A. G. Al-Gizi and S. J. Al-Chlahawi, "Study of FLC based MPPT in comparison with P&O and InC for PV systems," Proc. of IEEE International Symposium on Fundamentals of Electrical Engineering (ISFEE 2016), DOI: 10.1109/ISFEE.2016.7803187, ISBN: 978-1-4673-9575-5, Bucharest, Romania, 30 June-2 July, 2016, pp. 1-6.
- [4] A. Al-Gizi, A. Craciunescu, M. A. Fadel, and M. Louzani, "A new hybrid algorithm for PV MPPT under partial shading conditions," Rev. Roum. Sci. Techn.-Électrotechn. et Énerg., vol. 63, no. 1, 2018, pp. 52- 57.
- [5] Al-Gizi, A. Craciunescu, and S. J. Al-Chlahawi, "The use of ANN to supervise the PV MPPT based on FLC," Proc. of IEEE The 10th International Symposium on Advanced Topics in Electrical Engineering (ATEE 2017), DOI: 10.1109/ATEE.2017.7905128, ISBN: 978-1-5090-5160-1, Bucharest, Romania, March 23-25, 2017, pp. 703- 708.
- [6] A. G. Al-Gizi, M. Al-Saadi, S. Al-Chlahawi, A. Craciunescu, and M. A. Fadel, "Experimental installation of photovoltaic MPPT controller using Arduino board," Proc. of the IEEE International Conference on Applied and Theoretical Electricity (ICATE 2018), DOI: 10.1109/ICATE.2018.8551397, ISBN: 978-1-5386-3806-4, Craiova, Romania, October 4-6, 2018, pp. 1-6.
- [7] A.G. Al-Gizi and E. A. Hussein, "FPGA-based implementation of genetically tuned fuzzy logic controller (GA-FLC)," Journal of Engineering and Sustainable Development, vol. 16, no. 3, Sep. 2012, pp.241-257.[Online]. Available: <http://www.iasj.net/iasj?func=fulltext&aId=68292>
- [8] Y. A. Mohammed and L. K. Hashim, "Implementing fuzzy logic controller using VHDL," Eng. & Tech. Journal, vol. 25, no. 9, 2007, pp. 1049-1055.

[9] A. Al-Gizi, S. Al-Chlahawi, and A. Craciunescu, "Comparative study of some FLC-based MPPT methods for photovoltaic systems," *MATTER: International Journal of Science and Technology*, vol. 3, no. 3, 2017, pp. 36–50. DOI: 10.20319/mijst.2017.32.3650

[10] A. Al-Gizi, M. Louzazni, M. A. Fadel, and A. Craciunescu, "Critical constant illumination time in comparison of two maximum power point tracking photovoltaic algorithms," *U. P. B. Sci. Bull., Series C*, vol. 80, no. 2, Bucharest, Romania, 2018, pp. 201–216.

[11] S. Peng, "Modern digital designs with EDA, VHDL and FPGA," 1st edition, Terasic Inc., Jan. 2015.

[12] Quartus Prime lite software version 17.1. [Online]. Available:http://fpgasoftware.intel.com/17.1/?edition=lite&platform=windows&d_download_manager=dldm3

[13][Online].Available:
<http://www.abcsolar.com/pdf/bpsx150.pdf>

[14] C. Shih, "Floating-point to fixed-point conversion," 2004.

[15] H. Pant, H. Bourai, G. S. Rana, and S. C. Yadav, "Conversion of MATLAB code in VHDL using HDL coder & implementation of code on FPGA," *HCTL Open International Journal of Technology Innovations and Research (IJTIR)*, vol. 14, April 2015, pp. 1-9.

[16] W. Kleitz, "Digital electronics: a practical approach with VHDL," 9th edition, New York, 2012.